

Repolarization Alternans and Ventricular Arrhythmia in a Repaired Tetralogy of Fallot Animal Model

Shuenn-Nan Chiu, MD, PhD;* Chia-Ti Tsai, MD, PhD;* Lian-Yu Lin, MD, PhD; Shu-Chien Huang, MD, PhD; Yih-Sharnng Chen, MD, PhD; Jou-Kou Wang, MD, PhD; Mei-Hwan Wu, MD, PhD; Ling-Ping Lai, MD, PhD; Jiunn-Lee Lin, MD, PhD

Background—Ventricular arrhythmia is an important cause of late death in patients with repaired tetralogy of Fallot (rTOF). By using an rTOF canine model, we investigated the role of repolarization alternans and its electrophysiological mechanisms.

Methods and Results—Six dogs received right ventricular outflow tract (RVOT) transannular patch, pulmonary valve destruction, and right bundle branch ablation to simulate rTOF. After 1 year, we performed high-resolution dual-voltage and calcium optical mapping to record action potentials and calcium transients on the excised right ventricular outflow tract wedges. Another 6 dogs without operation served as control. The rTOF group was more susceptible to action potential duration alternans (APD-ALT) and spatially discordant APD-ALT than control (threshold for APD-ALT: 516 ± 36 vs 343 ± 36 ms; $P=0.017$; threshold for discordant APD-ALT: 387 ± 30 vs 310 ± 14 ms; $P=0.046$). We detected 2 episodes of ventricular tachycardia in the rTOF group, but none in the control. Expressions of Kv4.3 and KChIP2 decreased in the rTOF group. Expression of connexin 43 also decreased in the rTOF group with a corresponding decrease of conduction velocity and might contribute to spatially discordant APD-ALT. We also found distinct electrophysiological features of the RVOT, including biphasic relationship between magnitude of APD-ALT and pacing cycle length, uncoupling of APD-ALT, and calcium transients alternans, and shortened APD, but unchanged, APD restitution in rTOF.

Conclusions—We demonstrated novel electrophysiological properties of the RVOT. In an rTOF model, the RVOT exhibits increased susceptibility to temporal and spatially discordant APD-ALT, which was not totally dependent on calcium transient alternans. (*J Am Heart Assoc.* 2015;4:e002173 doi: 10.1161/JAHA.115.002173)

Key Words: action potentials • connexin 43 • ion channels • tachyarrhythmias • tetralogy of Fallot

Tetralogy of Fallot (TOF) is the most common cyanotic congenital heart disease, and surgical correction is necessary for patients to achieve long-term survival. However, after surgery, ventricular arrhythmia-related sudden cardiac death and right heart failure are still common late complications in these repaired TOF (rTOF) patients. It is one of the most common causes of right heart failure, even in the adult population.^{1–5} The mechanism of the ventricular arrhythmia in these rTOF has been studied for many years. Hemodynamic factors, including residual pulmonary regurgitation and result-

ing right ventricular outflow tract (RVOT) dilatation and right heart failure, could prolong QRS duration and result in ventricular arrhythmia in these rTOF patients. This mechano-electrical interaction is considered as the possible mechanism of ventricular arrhythmia in these patients.^{1,3,6,7} It is regarded as the model of ventricular arrhythmia in repaired congenital heart disease. The substrate of ventricular arrhythmia was also delineated at RVOT in previous studies.⁸ Although these studies have proved the mechano-electrical interaction in these rTOF patients, the exact mechanism of ventricular arrhythmia is still unclear.

The repolarization alternans and action potential duration alternans (APD-ALT) are crucial causes of dynamic wave instability, which may cause reentrant ventricular arrhythmia and sudden cardiac death.^{9,10} Calcium transient alternans (Ca-ALT), caused by sarcoplasmic reticulum calcium cycling, and a steeper action potential duration (APD) restitution slope have been proposed as possible mechanisms to explain the APD-ALT.^{10–12} Although several studies have examined these changes in the left ventricle, studies of APD-ALT, restitution, and Ca-ALT in the right ventricle are scarce and none in rTOF models. Recently, the importance of Ito (transient outward current) on the APD-ALT has gained much attention. In addition,

From the Departments of Pediatrics (S.-N.C., J.-K.W., M.-H.W.), Medicine (C.-T.T., L.-Y.L., L.-P.L., J.-L.L.), and Surgery (S.-C.H., Y.-S.C.), National Taiwan University Hospital, National Taiwan University, Taipei, Taiwan.

*Dr Chiu and Dr Tsai contributed equally to the article.

Correspondence to: Mei-Hwan Wu, MD, PhD, Department of Pediatrics, National Taiwan University Hospital, No. 7, Chung-Shan S. Rd, Taipei, Taiwan 100. E-mail: wumh@ntu.edu.tw

Received May 8, 2015; accepted October 23, 2015.

© 2015 The Authors. Published on behalf of the American Heart Association, Inc., by Wiley Blackwell. This is an open access article under the terms of the Creative Commons Attribution-NonCommercial License, which permits use, distribution and reproduction in any medium, provided the original work is properly cited and is not used for commercial purposes.

altered connexin expression has been documented as a substrate of ventricular arrhythmia in the dilated cardiomyopathy,¹³ but its role in the arrhythmia susceptibility of right ventricle has never been proved.

We have created a novel canine rTOF model by using RVOT incision with transannular patch creation, pulmonary valve destruction, and right bundle branch ablation.¹⁴ This model, with combined hemodynamic and electrophysiological factors, reflects adequately the clinical scenario of rTOF patients. We have proved the mechano-electrical interaction through this model, including significant progress of QRS duration prolongation, RVOT dilatation, and ventricular arrhythmia episodes.¹⁴ Here, using this novel rTOF animal model, we tried to delineate the cellular mechanisms of ventricular arrhythmia. We also tried to find the role of Ca-ALT, Ito, and connexin 43 in the genesis of ventricular arrhythmia.

Methods

Animal Preparation

The institutional animal study committee of National Taiwan University, College of Medicine approved this study (approval reference no.: IACUC 20110315), which complied with the National Academy of Science's "Guide for the Care and Use of Laboratory Animals." Nine canines younger than 1 year of age and weighing 10 to 12 kg were used as the study animals (rTOF group). They received the RVOT transannular patch creation, pulmonary valve destruction, and right bundle branch block (RBBB) creation to simulate rTOF as previously described.¹⁴ In brief, they received general anesthesia using intravenous virbac (2–3 mg/kg, Zoletil; Schering-Plough AB, Stockholm, Sweden) and xylazine (0.1–0.2 mg/kg, Rompun; Bayer, Leverkusen, Germany) as premedication. They were intubated with ventilator support. Electrocardiography (ECG) and blood pressure were monitored during the whole procedure. They received intravenous propofol (dose titration, Recofol; Bayer Schering, Turku, Finland) for deep general anesthesia to ensure no active motion and no increase of heart rate and blood pressure compared to the baseline. We performed the right bundle branch ablation using the transcutaneous radiofrequency catheter ablation method by 5 French MARINR catheters (Medtronic Inc, Minneapolis, MN). We then performed RVOT transannular whole-layer incision (around 3–4 cm in length, ie, from 0.5 to 1.0 cm above pulmonary valve to 2.5–3.0 cm below pulmonary valve), a surgical RVOT transannular patch, and pulmonary valve destruction through midline sternotomy after administration of succinylcholine (1 mg/kg, Relaxin; Kyorin, Taoyuan, Taiwan).¹⁴ After the procedures, we checked the ECG and pulmonary angiography to ensure the RBBB with prolonged QRS duration at the surface ECG and severe pulmonary regurgitation in pulmonary angiography.

Postoperative pain control was given with intramuscular carprofen (Rimadyl; Pfizer, New York, NY) and oral acetaminophen. Another 6 canines without operation served as control (control group). We implanted loop event recorders to detect arrhythmia episodes. We also performed electrophysiology study for ventricular arrhythmia inducibility at 6 months and 1 year after operation. The ventricular arrhythmia inducibility protocol was programmed ventricular stimulation at 2 right ventricular sites (typically apex and outflow tract) with 2 eight-beat drive trains (cycle lengths between 400 and 600 ms) and up to 4 extrastimuli with coupling intervals \geq 180 ms.

RVOT Wedge and Optical Mapping

One year after the intervention, under general anesthesia as previously described and midline sternotomy, the heart was quickly excised and the aorta was rapidly cannulated and perfused with a cold cardioplegic solution (Plegisol solution containing Ca 2.4 mEq, Mg 32 mEq, K 16 mEq, Na 110 mEq, Cl 160 mEq, and NaHCO₃ 0.01 mEq to maintain PH 7.4) for 3 minutes until no more blood could be washed out. RVOT preparations were taken from the base of the right ventricle (RV; approximate size of 3–4×4–8 cm in the rTOF group with previous incision line and patch included; Figure 1A). The right coronary artery was perfused and cannulated using a 4 French ARROW- Bermann catheter (Arrow International, Reading, PA; Figure 1B). In addition, endocardial tissue (<1 mm) was dissected from the RVOT adjacent to the wedge tissue and quickly frozen in –80°C for the ion channels and connexin study. We sutured around the RVOT wedges with silk to prevent small arterial leakage during perfusion. RVOT wedges were then mounted in a warmed chamber with the endocardial face up for endocardial optical mapping. We perfused the RVOT preparations with calcium containing Tyrode solution (gassed with 100% O₂, NaCl 136, KCl 5.4, MgCl₂ 1.0, CaCl₂ 1.8, NaH₂PO₄ 0.33, HEPES (4-(2-hydroxyethyl)-1-piperazineethanesulfonic acid 5.0, and a dextrose 10.0 solution; PH 7.4) at 37°C and arterial pressure of 50 to 70 mm Hg. Whole tissues were immersed in the perfusion efflux. Well-perfused RVOT wedges exhibit a reddish color and strong contractions with or without stimulation. Six canines in the study group and all 6 canines in the control group fulfilled the above criteria and were included in the subsequent study.

The prepared tissue wedges were then stained with Ca-sensitive dye Rhod-2 AM (4.5 μ mol/L; Molecular Probes Inc, Eugene, OR) 1 mg dissolved in 2 mL of DMSO containing Pluronic F-127 (20%) for 20 minutes. After another 15 minutes of Tyrode solution washout to de-esterificate Fluo-127, we directly injected voltage-sensitive dye RH237 (200 μ L dissolved in DMSO; Molecular Probes) into the perfusion system. We added blebbistatin (15 μ mol/L), a potent myosin II inhibitor, to avoid motion artifact during recording. Besides, we also covered

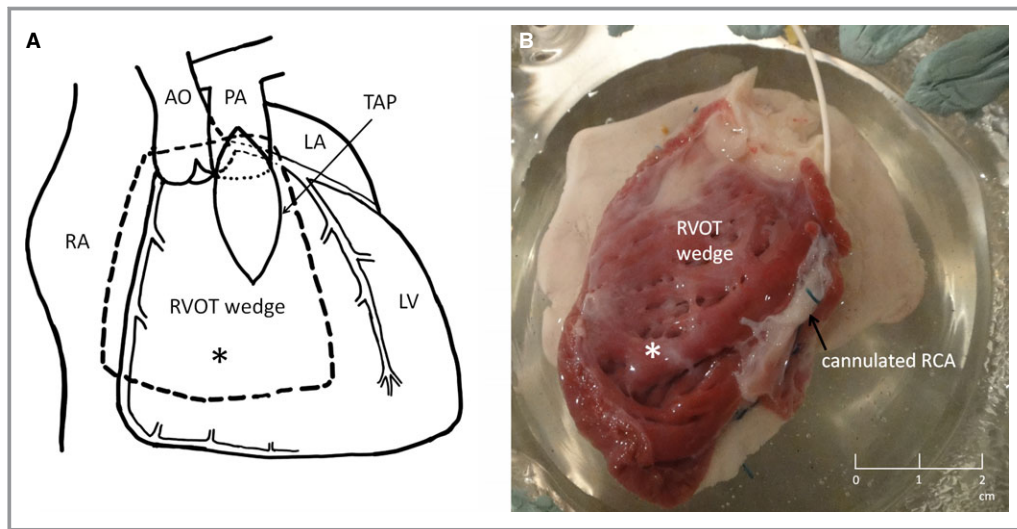


Figure 1. A, Illustration of the heart viewed from the anterior side. The dash line indicated the extent of RVOT wedge harvested in our study. The asterisk marked in the figure represents the stimulation site; (B) representative photograph of the endocardial surface of RVOT wedge (as dash line in A) in Langendorff perfusion system perfused by RCA in repaired tetralogy of Fallot animal. The asterisk marked in the figure represents the stimulation site. AO indicates aorta; LA, left atrium; LV, left ventricle; PA, pulmonary artery; RA, right atrium; RCA, right coronary artery; RVOT, right ventricular outflow tract; TAP, transannular patch.

1 glass on the RVOT wedge to overcome the uneven surface during optical mapping. Action potentials and Ca transients were recorded in the endocardial surface using 2 complementary metal-oxide-semiconductor cameras (MiCam Ultima; Sci-Media, Tokyo, Japan), each with 100×100 pixels and acquiring images at 1000 frames/s.^{15–17} Fluorescent light from both dyes was split by a fluorescence splitter (MiCam Ultima; Sci-Media). The longer-wavelength light (690 nm), for action potential recording, and shorter-wavelength light (585 nm), for Ca transient recording, was directed at the 2 CMOS cameras.

Electrophysiological Protocols

The pacing electrodes were placed and fixed at the most apical site of RVOT (Figure 1). We performed baseline pacing at pacing cycle length 1000 ms. Thereafter, we gave burst pacing for 20-beat drive trains with pacing cycle length (PCL) 800, 700, and 600 ms, and then decreased gradually at 20 ms step till conduction block or till PCL 200 ms. We took a 30-second break between each PCL for calcium transient recovery.

Measurement of Conduction Velocity, APD-ALT, Ca-ALT, and APD Restitution

Conduction velocity was calculated at baseline pacing cycle length 1000 ms according to the previous report.¹⁸ We determined APD-ALT by measuring the differences of even and odd beats in local APD on 6 consecutive beats according to our previously reported method.¹⁵ The APD-ALT was plotted against the PCL. Dynamic APD restitution was measured by

plotting APD as a function of the diastolic interval. The restitution curve was fit to a single exponential function, where the time constant, τ , was used to measure the kinetics of APD restitution. The spatial patterns and gradients of repolarization, or magnitude of APD-ALT, were represented as iso-alternans contour maps.

The calcium level was reported as F/F_0 , where F_0 was the resting or diastolic fluorescence level. To quantify Ca-ALT, the difference in the net amplitude of the larger and smaller calcium transient was expressed as a percentage of the net amplitude of the larger transient according to our previously reported method.¹⁴ PCL at which change of F/F_0 more than 20% on consecutive beats was defined as the PCL threshold to induce Ca-ALT. Measurements were made on 6 serial consecutive beats, and the F/F_0 was averaged for the 3 even and 3 odd beats, respectively. All of the above electrophysiology studies were completed within 2 hours to avoid hypoxia because of prolonged experiments.

mRNA Expression of Connexin 40, 43, and Ion Channels

Tissues were harvested and RNA was extracted using TRI Reagent Solution (Ambion Inc, Austin, TX). Single-stranded cDNA synthesis was performed using the High Capacity cDNA Reverse Transcription Kit (Applied Biosystems Inc, Foster, CA). Polymerase chain reaction (PCR) primers were designed using Primer Express V.2.0 software (Applied Biosystems). Primer sequences used in this study are shown in Table. Human 18S ribosomal RNA was used as endogenous control. Real-time PCR

was carried out in a MicroAmp Optical 96-well plate using power SYBR Green PCR Master Mix (Applied Biosystems), with 2 μ L of cDNA in each well. PCR reactions were monitored in real time using the ABI 7900HT Fast Real-time PCR system (Applied Biosystems). The thermal cycling conditions for real-time PCR were 50°C for 2 minutes, then 95°C for 10 minutes, and 40 cycles of denature (95°C, 15 seconds) and annealing/extension (60°C, 60 seconds). After PCR cycles, a dissociation curve examination was performed. Relative quantization of gene expression was determined using the $\Delta\Delta$ Ct method.¹⁹

Statistical Analysis

All data are expressed as mean \pm SEMs. Data from the independent group were compared using the nonparametric Wilcoxon rank-sum test for continuous data and the Fisher exact test for categorical data. $P<0.05$ was considered statistically significant.

Results

Basic Hemodynamic Data, Electrophysiological Characteristics, and Ventricular Arrhythmia Susceptibility

Severe pulmonary regurgitation was documented by echocardiography in all 9 dogs. RVOT diameters increased signifi-

cantly from 7.9 ± 0.8 to 17.5 ± 2.1 mm 1 year after operation in the rTOF group ($P<0.001$). Extensive fibrosis was noted in the surgical epicardial region of the RVOT. The surface EKG showed a longer QRS duration and QTc interval in 9 dogs in the rTOF group compared to the 6 dogs in the control group (QRS duration: 103.6 ± 5.4 vs 54 ± 5.1 ms; $P<0.001$; QTc interval: 363.2 ± 17.7 vs 310.0 ± 15.3 ms; $P=0.001$). However, the JTc interval was shorter in the rTOF model than control, although not statistically significant (222.6 ± 13.9 ms in the rTOF group vs 239 ± 12.6 ms in the control group; $P=0.413$). Ventricular tachycardia events were common and half of the dogs in study animals had more than 5 episodes of short-run ventricular tachycardia within 1 year of recording. For electrophysiology study, ventricular arrhythmia could be induced in 1 of 7 at 6 months and 1 of 6 at 1 year after operation.

Optical mapping data were available in 6 of 9 dogs and indicated shorter APD in the rTOF group compared to the control group (Figure 2), which corresponded to a shorter JTc interval in the rTOF group. At pacing with a PCL of 500 ms, the APD85 was 234 ± 12 ms in the rTOF group and 263 ± 23 ms in the control group ($P=0.052$). For the wedge preparations, among the 6 dogs of the rTOF group, 1 had spontaneous ventricular tachycardia (VT) at the beginning of optical mapping study, which was then converted by defibrillation. Another exhibited polymorphic VT during burst ventricular pacing at PCL 200 ms. The polymorphic VT then transformed to monomorphic VT spontaneously (Figure 3A).

Table. Primer Sequence for Real-Time Polymerase Chain Reaction in This Study

Dog KCHIP2	Forward	CATGGAGTGAGTCAGGGACCAT
	Reverse	ACTTCCCTCCTTCCCCTTTCT
Dog KCNH2	Forward	CCTTCGACTTGCTCATCTTTGG
	Reverse	CTTCAGCAGCCGATCAGTT
Dog CAV1.2	Forward	CATGTTTCGCTGCATTGG
	Reverse	TTTGGAACATCTGAACAGGTGTAGAG
Dog KCNQ1	Forward	TCCCTTTCATCTCCGTCTCA
	Reverse	TGCCCAATCGTGTGCT
Dog NAV1.5	Forward	ACAGCTGGAACATCTTCGACTTT
	Reverse	GAGAGCACGGTACCCACGAT
Dog kir2.1	Forward	TCTTCGAGGAGAAGCATACTACAAA
	Reverse	TTGGGCACTTCGTAGGTCTTG
Dog Cx40	Forward	GACCCTCGGCTGGCATAGT
	Reverse	GGCCATTTTCCAGACACTGATT
Dog Cx43	Forward	CCTGCTGCGAACCTACATCA
	Reverse	AAGGCCACCTCGAAAACAG
Dog Kv4.3	Forward	CCTGCTGCTCCCGTCGTA
	Reverse	AGTGGCTGGCAGGTTGGA

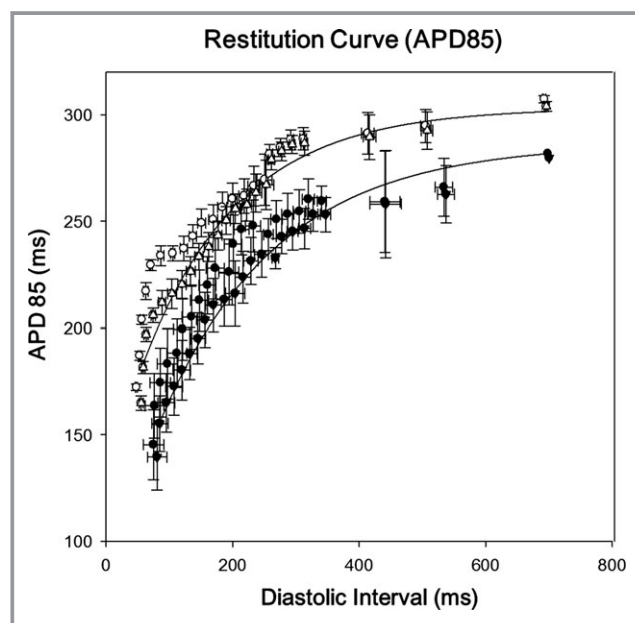


Figure 2. Comparison of the dynamic restitution curve between the 6 dogs in repaired tetralogy of Fallot group (solid circle) and the 6 dogs in the control group (blank circle). The maximal restitution slope was not significantly different between the 2 groups. APD indicates action potential duration.

Conversely, the control group exhibited no spontaneous or inducible ventricular arrhythmia. However, the activation map of the beat just before VT did not show reentry circuit and conduction block (data not shown), probably because that the mapping region was a passive site, not the exact site of conduction block or re-entry.

Increased Repolarization Alternans in the rTOF Model

The temporal APD-ALT (defined as APD-ALT >10 ms) began at a longer PCL in the rTOF group compared to the control group (Figure 4A), indicating an increased susceptibility to APD-ALT in the rTOF group. Onset of APD50 and APD85 alternans (>10 ms) was 516 ± 48 and 516 ± 36 ms in the rTOF group, which were significantly longer compared to the control group (360 ± 22 and 343 ± 36 ms; $P=0.030$ and 0.017 , respectively). The relationship between the magnitude of APD-ALT and the PCL is shown in Figure 4A. In both groups, the APD-ALT increased with decreasing PCL. However, when the PCL shortened further, the APD-ALT decreased conversely. This biphasic phenomenon was even more prominent in the rTOF group. The APD85 alternans began to drop at a pacing cycle length of 380 ms in the rTOF group. However, when the pacing cycle length decreased further, the phase 1 notch disappeared and the APD-ALT became less prominent (as shown at pacing cycle length 220 ms; Figure 3B, left panel).

Ca-ALT has been proposed as one of the major mechanisms contributing to APD-ALT.^{10–12} We performed dual-voltage and calcium mapping experiments to evaluate the relationship between APD-ALT and Ca-ALT at various PCLs in the rTOF group and the control group. Figure 3C shows that at the PCL of 600 ms, Ca-ALT was prominent in the rTOF group, but not significant in the control group. This phenomenon was observed with decreasing PCL until 420 ms (not shown in the figure). Onset PCL of Ca-ALT was longer in the rTOF group (435 ± 61 ms) compared to the control group, but not statistically significant (320 ± 18 ms; $P=0.114$; Figure 4B).

However, we noticed that occurrences of APD-ALT and Ca-ALT were not closely coupled and were independent, especially in the rTOF groups. For example, the site with maximal APD-ALT was not associated with maximal Ca-ALT and vice versa (Figure 3B and 3C). Numerous locations with significant APD-ALT exhibited no corresponding significant Ca-ALT (Figure 5A and 5C), and numerous locations with significant Ca-ALT exhibited nonsignificant APD-ALT (Figure 5B and 5D). The biphasic phenomenon of the relationship between APD-ALT and PCL was not shown in the relationship between Ca-ALT and PCL either. The correlation of APD-ALT and Ca-ALT were significant at PCL longer than 400 ms both in rTOF and control group (correlation coefficients 0.791 and 0.895; $P=0.002$ and <0.001 , respectively). However, at PCL less

than 400 ms, the correlation became nonsignificant (correlation coefficients -0.577 and -0.473 in the rTOF and control group; $P>0.05$). These findings are distinct from the observation of a previous study, in which the APD-ALT was dependent on Ca-ALT in the canine left ventricular wedge preparations.²⁰

Spatial Repolarization Heterogeneity in the rTOF Model

Spatially discordant APD-ALT, which produces a large repolarization gradient, is the most malignant spatial repolarization heterogeneity and provides the substrate of conduction block and re-entry. Therefore, discordant APD-ALT is a sensitive marker of susceptibility to ventricular arrhythmia or sudden cardiac death.^{21,22} In our study, we found that spatially discordant APD-ALT was shown in both the rTOF and control groups (3 of the rTOF group and 2 of the control group; $P>0.05$). However, the threshold for discordant alternans occurred at longer PCL in the rTOF group compared to the control group (387 ± 30 vs 310 ± 14 ms; $P=0.046$), indicating an increased susceptibility to discordant alternans. Furthermore, only in the rTOF group, but not in the control group, we found discordant APD-ALT between close adjacent sites. This may create a large repolarization gradient and provide a primary substrate for re-entrant arrhythmia (Figure 6). We could observe significant discordant alternans at pacing cycle length of 320 ms in the rTOF RVOT preparation, because the APD of myocytes alternates with the opposite phase between adjacent sites, depicted by the presence of both red and blue contours. In the control group, the in-phase alternans (concordant alternans) is distributed across the entire map region.

We noticed that the discordant APD-ALT was not dependent on discordant Ca-ALT in the RVOT wedges. Numerous sites with discordant APD-ALT showed no discordant Ca-ALT (Figure 5C), and numerous sites with discordant Ca-ALT showed no corresponding discordant APD-ALT (Figure 5D). This suggested that the discordant APD-ALT mechanism was not calcium dependent.

We also compared the APD dispersion in the rTOF and control group as shown in representative contour maps of APD (Figure 7). However, we did not find any significant difference in the APD dispersion in the endocardial optical mapping between these 2 groups.

Restitution Curve Slope and Time Constant in the rTOF Model

Because the mechanism of APD-ALT is not totally dependent on Ca-ALT in the RVOT wedges, we checked the restitution curve characteristics in both the rTOF and control groups

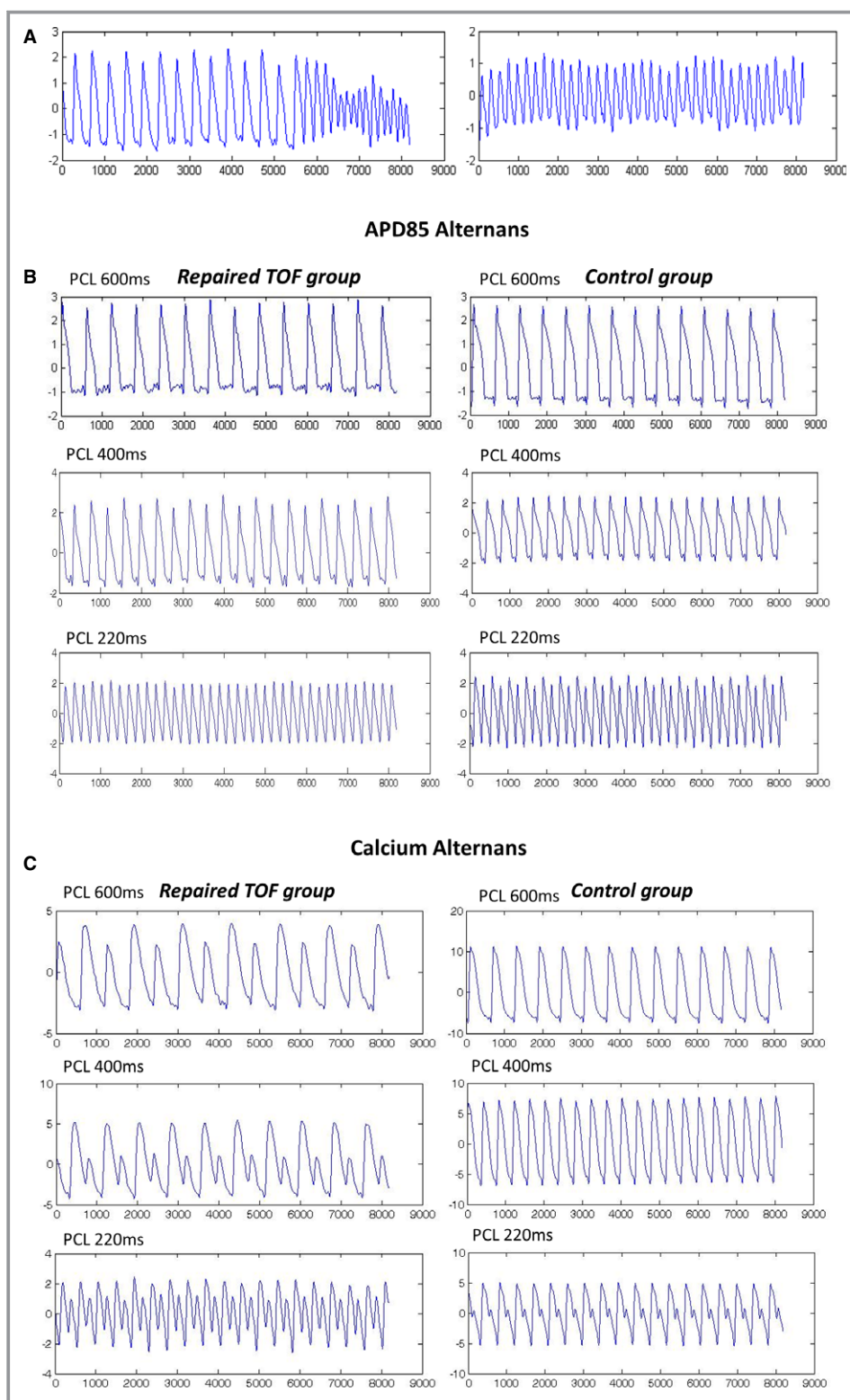


Figure 3. A, Polymorphic VT induced by rapid pacing, which then shifted to more organized monomorphic VT (right panel). The units of the y axis are arbitrary units. B, Representative action potentials at the same site during the pacing cycle length of 600, 400, and 220 ms in the repaired TOF group (left panel) and the control group (right panel). (C) Representative calcium transient at the same site at pacing cycle length 600, 400, and 220 ms (at the same site corresponding to the action potential duration above) in the repaired TOF (left panel) and control group (right panel). APD indicates action potential duration; PCL, pacing cycle length; TOF, tetralogy of Fallot; VT, ventricular tachycardia.

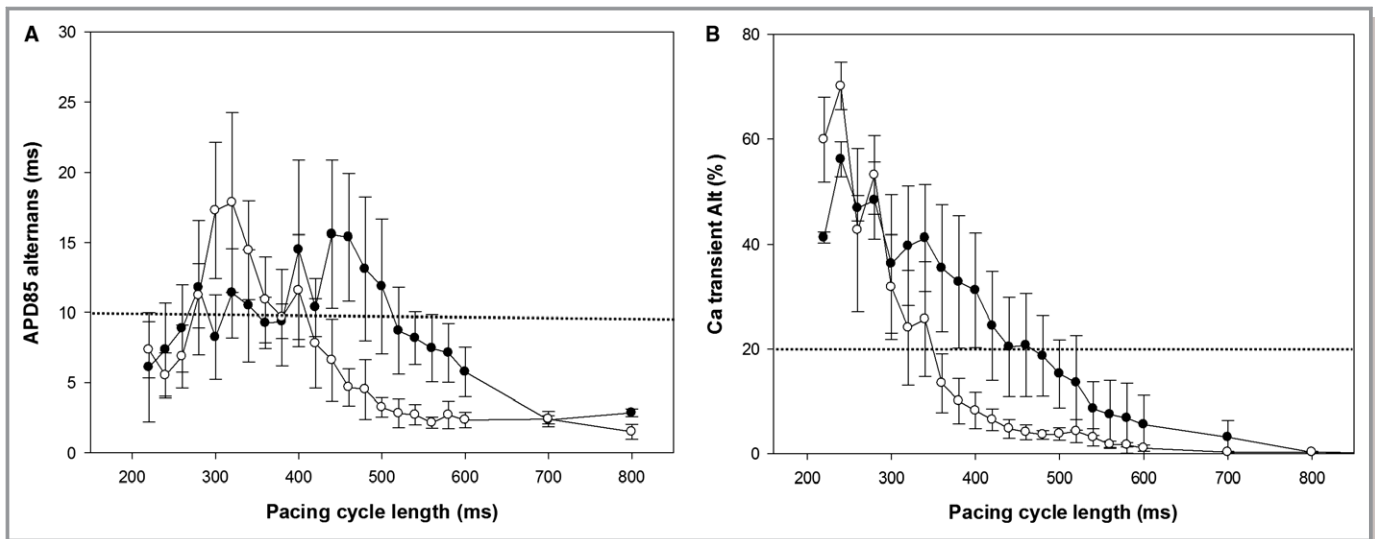


Figure 4. A, Relationship of APD 85 alternans and pacing cycle length in the repaired TOF (solid circle) and control group (blank circle). The onset pacing cycle length of action potential alternans (>10 ms) in the repaired TOF group was significantly longer than that in the control group (516 ± 36 vs 343 ± 36 ; $P=0.017$). B, Relationship of calcium transient alternans and pacing cycle length in the repaired TOF (solid circle) and control group (blank circle). The onset pacing cycle length of calcium transient alternans (>20%) in the repaired TOF group was longer than the control group, but not statistically significant (435 ± 61 vs 320 ± 18 ms; $P=0.114$). APD indicates action potential duration; TOF, tetralogy of Fallot.

(Figure 2), because a steeper APD restitution may contribute to susceptibility to APD-ALT.^{10–12} Although the APD was shorter in the rTOF group, the maximal slope of restitution

curves was not significantly different between the 2 groups. The time constant, τ , was 126.6 ms in the rTOF group and 140.8 ms in the control group ($P>0.05$). The maximal slope of

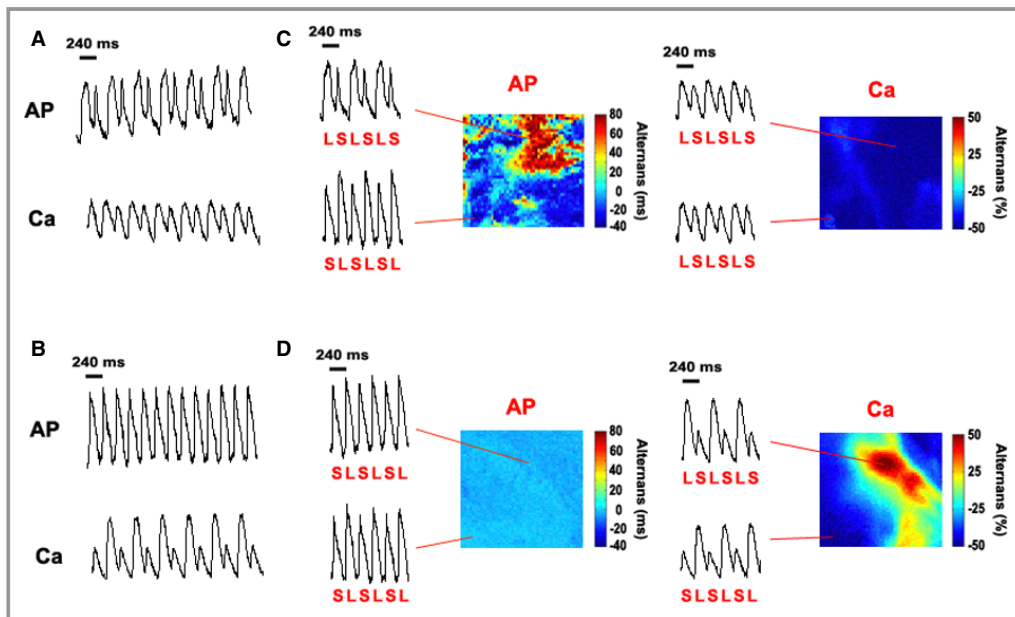


Figure 5. A, In one location of the representative right ventricular outflow tract preparation, the AP shows significant alternans at pacing cycle length 300 ms, but not calcium transients alternans. B, Another location of the same right ventricular outflow tract preparation shows significant Ca-ALT, but no significant APD-ALT. C, The contour map also shows a mismatch of APD and Ca distributions. D, Discordant Ca-ALT was unassociated with discordant APD-ALT. AP indicates action potentials; APD-ALT, action potential duration alternans; Ca-ALT, calcium alternans; L, long APD or large Ca; S, short APD or small Ca.

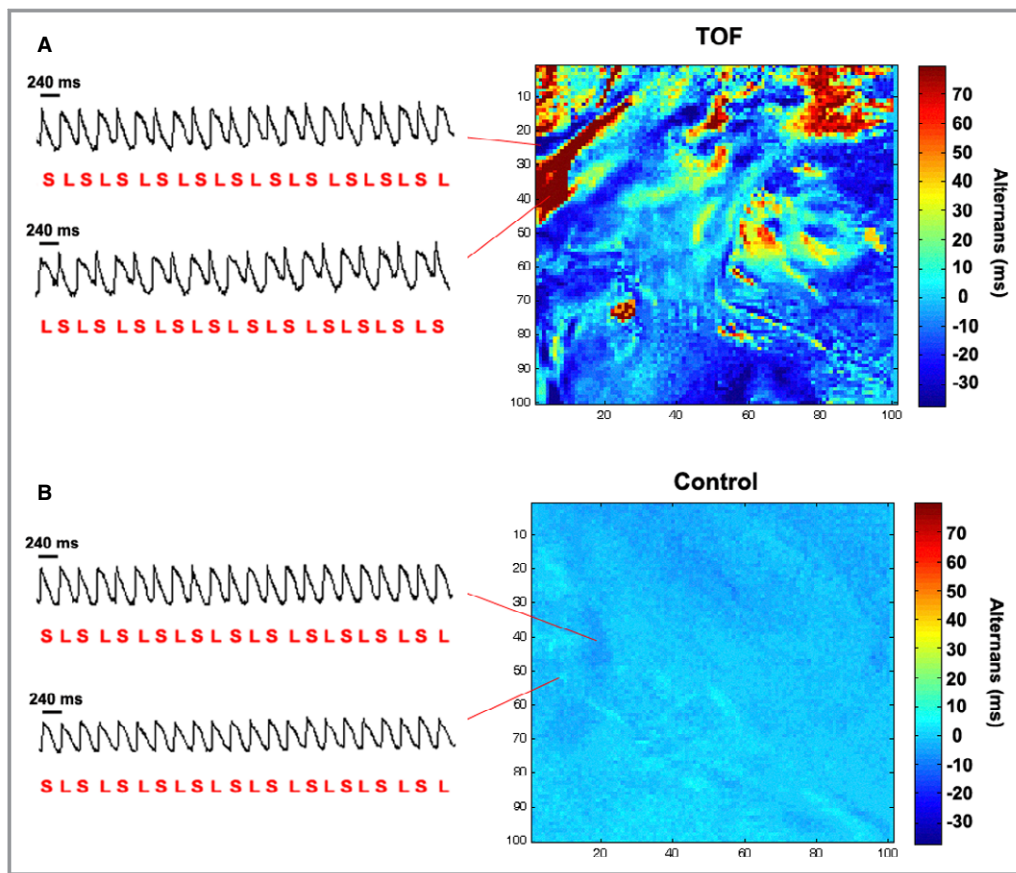


Figure 6. A, The contour map of repaired TOF right ventricular outflow tract preparation shows the APD-ALT magnitude (contour intensity), which is out of phase between adjacent sites (discordant alternans) at a pacing cycle length of 320 ms, creating a large repolarization gradient and providing the substrate for re-entrant arrhythmia (contour color: red is+phase [long and short APD alternation], blue is−phase [short and long APD alternation]). B, The control preparation shows the in-phase alternans (concordant alternans) between the adjacent sites at 320 ms pacing cycle length. APD-ALT indicates action potential duration alternans; TOF, tetralogy of Fallot.

the restitution curve (APD85 vs the diastolic interval) was 0.88 ± 0.10 in the rTOF group and 0.88 ± 0.12 in the control group ($P=0.931$).

Decrease Conduction Velocity and Down-Regulation of Connexin 43 in the RVOT of the rTOF

Because the discordant APD-ALT in the RVOT wedges was not totally dependent on calcium or steeper APD restitution curve, we checked the connexin expression in the RVOT wedges. Decreased cell-cell coupling has been proposed as an important mechanism of spatially discordant APD-ALT.^{13,23,24} The results are shown in Figure 8A. We found lower mRNA expression of connexin 43 in the RVOT wedges of the rTOF group. For connexin 40, mRNA expression level was similar between the 2 groups.

We then delineated whether decreased connexin 43 levels in the rTOF wedges were associated with a corresponding functional change, that is, slower conduction, which would also provide a substrate for re-entrant arrhythmia. We found that the averaged conduction velocity was lower in the rTOF wedges, compared to that of the control wedges (44.5 ± 6.4 vs 35.3 ± 5.7 cm/s; $P=0.025$). The decreased conduction velocity in the rTOF wedges was in accord with the finding of increased QRS duration in the rTOF wedges. Figure 8B and 8C shows the representative activation maps of the rTOF wedges and the control wedges. The activation map of the control wedge showed uniform conduction path. However, the activation map of the rTOF wedge showed heterogeneous conduction patterns with areas of slow conduction and curvature of conduction wave fronts, providing the substrate of conduction direction change and re-entrant arrhythmia.

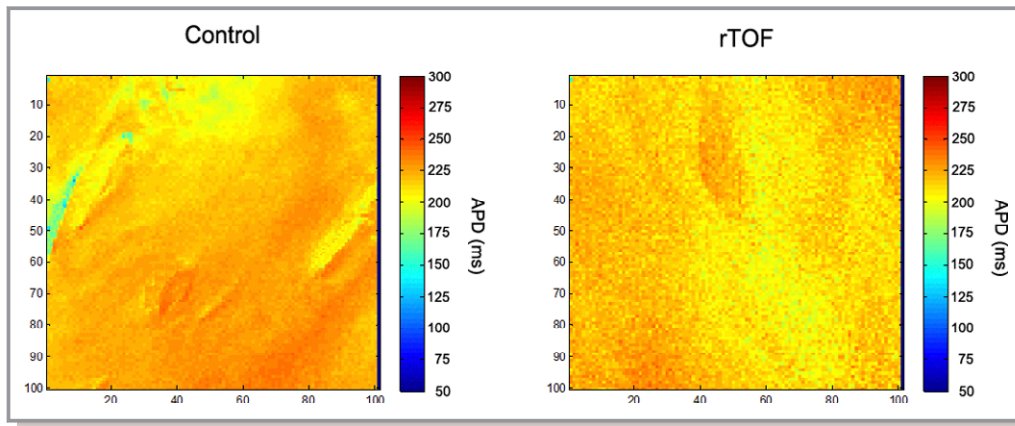


Figure 7. Representative contour maps of APD in the endocardial surface at pacing cycle length 500 ms between the rTOF group and control. We can see that the APD dispersion did not show a significant difference between the 2 groups. APD indicates action potential duration; rTOF, repaired tetralogy of Fallot.

Down Regulation of Ito and Other K Channel Expression in the RVOT of rTOF

Because the transient outward current was more prominent and could be an important cause of APD-ALT in the RVOT, we first checked the Kv4.3 (which is the main Kv gene encoding for α subunit of the RVOT Ito channel) and KCHIP2 (K channel interacting protein 2, which forms β subunit and regulating Kv4.3 gene expression) mRNA expressions in the RVOT of the rTOF and control group. We found the Kv4.3 and KCHIP2 mRNA expressions were lower in the rTOF group, compared to the control group, with borderline statistical significance (Figure 9; $P=0.054$ and 0.05 respectively).

We also checked mRNA expressions of the other ion channels in the rTOF and control group as shown in Figure 9. We could observe general down-regulation of sodium, potas-

sium, and calcium channel, especially in the KCNQ1 channel which reached statistically significant difference ($P=0.05$).

Discussion

In this systemic and extensive electrophysiological study, by using a novel rTOF canine model, we observed (1) the spatial and temporal repolarization heterogeneities are common, and could be the underlying mechanism of increased susceptibility to ventricular arrhythmia in rTOF; (2) the APD-ALT was not totally dependent on Ca-ALT or APD restitution, but the mechanisms may be multiple related to the associated findings of connexin 43 and Ito down-regulation; (3) in contrast to APD prolongation in the failure left ventricle, shortened APD was found in failure RVOT from rTOF canines; (4) general down-regulation of cardiac ion channels especially

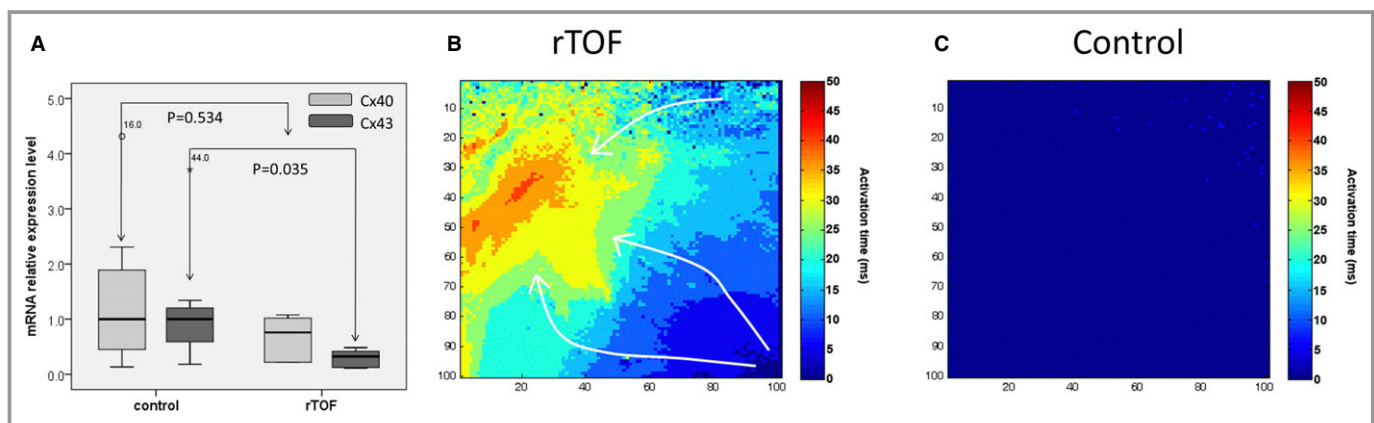


Figure 8. A, mRNA expression level of the connexin 40 and 43 between the 6 dogs in the repaired tetralogy of Fallot (rTOF) group and 6 dogs in the control groups. Connexin 43 expression was significantly lower in the rTOF group than the control group, but not connexin 40 expression. (B) Representative activation maps for the rTOF group and (C) control group are shown. In the representative rTOF group, in addition to conduction slowing, the activation map also shows heterogeneous conduction patterns with curvature of conduction wave fronts (white arrows). In the representative control group, the conduction is very fast and homogeneous.

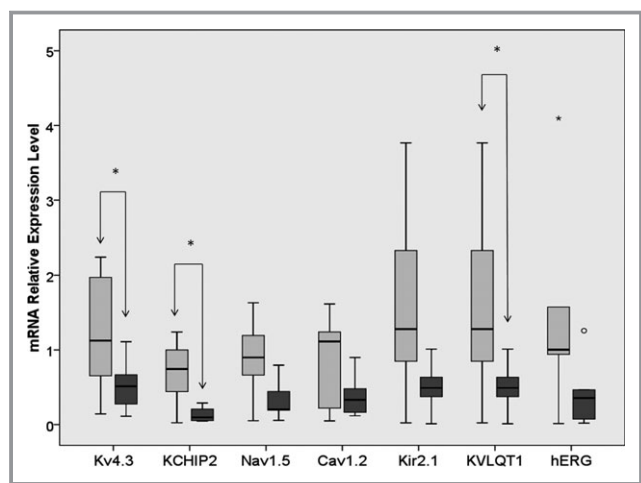


Figure 9. Relative mRNA expression level of the Kv4.3, KCHIP2, Nav1.5, Cav1.3, KCNQ1, and KCNH2 between the 6 dogs in the repaired tetralogy of Fallot (rTOF) group and 6 dogs in the control groups. The Kv4.3, KCHIP2, and KCNQ1 expression was lower in the rTOF group than the control group. Light gray, control; dark gray, rTOF group. * $P=0.05$.

Kv4.3, KCHIP2, and KCNQ1 was present in the RVOT of our rTOF model, a finding of ionic channel remodeling similar to left heart failure.

Role of Repolarization Heterogeneity in rTOF

For the rTOF patients, previous studies had shown right ventricle dilatation and impaired right ventricular function were common in addition to severe pulmonary regurgitation.^{25,26} In our rTOF model, right ventricle dilatation is also consistently found.¹⁴ Besides, right ventricular failure is associated with ventricular arrhythmia and mortality.^{25,27} These findings are similar to those in left heart failure. For the mechanism of ventricular arrhythmia in rTOF, the role of repolarization abnormality on the genesis of ventricular arrhythmia in rTOF patients is increasingly recognized recently.^{1,7,14} Khairy et al. showed that although monomorphic VT was more frequently induced at electrophysiological study, patients with inducible polymorphic VT had the highest risk of late ventricular arrhythmia and sudden cardiac death during follow-up.²⁸ They further showed that repolarization heterogeneity might increase susceptibility to ventricular arrhythmia and sudden cardiac death. Besides, RVOT was found to be the main substrate of ventricular arrhythmia in these rTOF patients.⁸ In our previous study, we had demonstrated a higher microvolt T-wave alternans value, which is a marker of repolarization heterogeneity, in rTOF patients, especially in those with previous ventricular arrhythmia episodes.¹

Repolarization heterogeneity is also an essential mechanism for monomorphic VT. In one animal study evaluating the

ventricular arrhythmia in the myocardium with a structural barrier by the optical mapping method, electrical stimulation often induced monomorphic VT in the presence of repolarization heterogeneity.²⁹ Because surgical scar (a structural barrier) is always present in rTOF patients, monomorphic VT is therefore more likely induced, which may explain more monomorphic VT in these rTOF patients. In the present study, one of the rTOF canines had induced polymorphic VT initially, which then spontaneously transformed to monomorphic VT. Although the activation map for the beat initiating VT did not show conduction block or re-entry circuit, the plausible explanation may be that the mapping site was a passive site and not necessarily the site in which conduction block or reentry occurred.

In the present study, using a novel rTOF animal model, we further observed that APD-ALT occurred at lower heart rates in rTOF canines than in the controls. Discordant alternans also occurred at lower heart rates, and the extent was more severe in the rTOF canines. Therefore, the temporal and spatial repolarization heterogeneities were more prominent in rTOF canines, as compared to controls. These results support that augmented repolarization heterogeneity is likely a crucial mechanism of ventricular arrhythmia in rTOF patients.

Mechanism of Increased Susceptibility to Repolarization Heterogeneity in rTOF

To address the role of calcium in the mechanism of repolarization heterogeneity in rTOF, we are the first group to perform dual-voltage and calcium mappings in the RVOT wedges. Surprisingly, we did not identify crucial role of calcium alternans in the mechanism of susceptibility to APD-ALT in the RVOT from the rTOF group, especially at shorter PCL. Previous studies in the canine left ventricular wedges have shown that APD-ALT is driven by the Ca-ALT. The failure left ventricular wedges are more susceptible to Ca-ALT and thus more susceptible to APD-ALT and re-entrant arrhythmia.^{10,11,20,22} The action potentials and calcium transients are typically coupled.^{20,30,31} We demonstrated the distinct electrophysiological characteristics of RVOT, which had never been described. The changes of action potentials of RVOT were not perfectly coupled with the changes of calcium transients.

Steep electrical restitution also plays a crucial role in the susceptibility to APD-ALT at high rates in left ventricular wedges.^{12,32} In the RVOT preparations, we also did not observe differences in the electrical restitution properties between the rTOF and control groups. Even, in the RVOT from the rTOF group, the restitution curve remained unchanged and did not become steeper. All these electrophysiological properties of RVOT are distinct from those of the left ventricle, and never been described, either.

Biphasic Phenomenon of the Relationship Between PCL and APD-ALT

In this RVOT electrophysiological study, we observed a biphasic phenomenon in the relationship between PCL and alternans magnitude, particularly in the rTOF group. Similar findings had been described in the RVOT of the canine animal model of Brugada syndrome, in which the T-wave alternans occurred initially at long PCL 3000 to 600 ms. However, when the PCL decreased further, the T-wave alternans disappeared.³³ Such biphasic phenomenon in the relationship between PCL and alternans magnitude may involve the Ito current, which behave similarly in a biphasic pattern, with decreased alternans magnitude at higher rates.³⁴ In Luo-Rudy simulating phase 1 model in the left ventricle, they found that the Ito governed APD-ALT in the middle range of pacing cycle length.³⁵ Because the Ito current is particularly abundant in RVOT tissue, it is highly possible that in the RVOT, the mechanism of APD-ALT is partially dependent on the kinetics of sarcolemmal Ito current and is not driven by calcium dynamics alone. This is in contrast to the previous studies in the left ventricular tissues, in which the APD-ALT is driven by calcium kinetics.^{16,21}

In the normal RVOT of our control animal, we found the prominent phase 1 notch in alternating beats (eg, PCL 220 ms at Figure 3B right panel). This phase 1 alternans, which is controlled by Ito currents, existed even at short pacing cycle length.^{36,37} In contrast, in the rTOF model, the phase 1 alternans (Ito alternans) begin at longer PCL, probably collaborating with Ca-ALT, contributes to the earlier onset of APD-ALT. The earlier onset of Ito alternans may be attributable to change of Ito kinetics. However, at shorter pacing cycle length, the phase 1 notch is less prominent and phase 1 alternans disappear in the rTOF group. This phenomenon is caused by the decreased Ito mRNA expression and may be the reason of more-prominent biphasic phenomenon in the rTOF group. Interestingly, down-regulation of Ito expression as we have shown in the rTOF group, is also commonly found in left heart failure models.^{38,39} In addition, given that Ito down-regulation is often heterogenous in heart failure, it may cause discordant alternans in our rTOF model. This also contributes to the mechanism of ventricular arrhythmia.

Decrease Conduction Velocity and Expression of Connexin 43 in rTOF Canines

Decreased connexin 43 expression and slower conduction velocities have been demonstrated in left heart failure.¹³ In the present study, we also demonstrated slower conduction velocity and decreased connexin 43 expression in the RVOT of rTOF. The effect of decreased connexin 43 expression in the

rTOF is 2-fold. First, because connexin 43 is the major gap junction protein in the ventricle, lower connexin 43 expression can reduce gap junction function and cause uncoupling of ventricular myocytes and reduce conduction velocity. Slower conduction may result in conduction block and initiation of re-entrant arrhythmia.^{13,23} Second, uncoupling of ventricular myocytes is also the main cause of spatially discordant APD-ALT. It can then increase susceptibility to functional conduction block and initiation of re-entrant arrhythmia.⁴⁰ This may be a critical component of the arrhythmia substrate for the slow conduction zone and conduction block. The effect of decreased connexin 43 expression, together with scar-related myocardial fibrosis, which has been demonstrated in previous studies,²⁶ plays a critical role in the mechanism of increased susceptibility to ventricular arrhythmia in the rTOF.

Shorter APD in RVOT Failure of rTOF Canines

In the left ventricular heart failure model, general down-regulation of ion channels, especially K channels, is common. Among these channels, Ito current down-regulation is the most consistent ionic current change in failing hearts.^{41,42} In the present study, we also found general down-regulation of ion channels, especially Kv4.3, KChIP2, and KCNQ1, in the rTOF group. This result may imply that rTOF is a kind of right ventricular failure.

In our study, the QRS duration and QTc interval was prolonged in the rTOF group. This is related to the bundle branch block, which is a common finding after TOF corrective surgery, and may also cause RV desynchronized contraction.⁴³ However, the JTc interval and APD were shortened in our rTOF canines. In left ventricular heart failure, APD was reported to be heterogeneously prolonged.²³ For RV heart failure, Benoist et al. reported that the QT and APD were also prolonged in an animal model of RV failure caused by monocrotaline-induced pulmonary hypertension.⁴⁴ We are the first group to focus on the electrophysiological characteristics of the failure RVOT and found a contradictory change of shortened APD. In the left failure heart, both outward potassium current (IK) and L-type calcium current (ICaL) would decrease.^{41,45} Decreased IK is often more prominent than decreased ICaL, with a net effect of decreased outward current and prolonged APD.⁴¹ In contrary, in the right heart failure, down-regulation of Ito current in the rTOF model may decrease the ICaL and Na-Ca exchanger-induced calcium influx in large animals and caused APD shortening.^{36,37}

Study Limitations

The primary limitation of this study is the relatively small number of study animals. Because of the difficulties of the

surgical procedure, postoperative care for rTOF canines, and extending study period for more than 1 year to simulate the clinical scenario, we could enroll a relatively small number of experimental animals. Second, because the operative procedure, including RVOT incision and transannular patch, is necessary to create the rTOF model, the inevitable adhesion and extensive fibrosis of RVOT epicardium cause the RVOT epicardium optical mapping to be impossible. We mapped the endocardial region in which no significant fibrosis was noted, and therefore the APD dispersion did not show any difference in the endocardial surface between the 2 groups. We know that the scar or fibrosis is also important in the mechanism of arrhythmogenesis in RVOT. However, the mechanism of scar-related predisposition to ventricular arrhythmia has been well documented, and we sought to identify mechanism(s) other than scar or fibrosis, including APD-ALT, connexin 43 down-regulation-related conduction velocity slowing, and Ito down-regulation. These factors, in combination with fibrosis, cause the susceptibility to ventricular arrhythmia in repaired TOF patients. Third, because the major aim of the present study was the long-term effect of TOF on arrhythmia mechanisms (1 year after operation), which may be not interfered with by the sham procedures 1 year ago, we did not perform the sham operation.

Conclusion

The RVOT shows distinct electrophysiological features, such as the biphasic relationship between magnitude of APD-ALT and PCL, uncoupling of APD-ALT, and Ca-ALT. The RVOT from rTOF, or failure RVOT, shows shortened APD, an increased susceptibility to develop APD-ALT, and spatially discordant APD-ALT and thus an increased susceptibility to ventricular arrhythmia. The mechanism of increased susceptibility to APD-ALT is not through calcium transient dynamics alone, but also related to multiple factors that still remain elusive in the current study, such as changing kinetics of Ito current and decreased connexin 43 expression and resulting slow conduction velocity with cell-cell uncoupling.

Acknowledgments

This work was supported, in part, by the National Taiwan University College of Medicine Laboratory Animal Center.

Sources of Funding

This work was supported by the National Taiwan University Hospital (Grant No.: NTUH.101-M1935) and National Science Council in Taiwan (Grant No.: 104-2314-B-002-167-MY3).

Disclosures

None.

References

1. Chiu SN, Chiu HH, Wang JK, Lin MT, Chen CA, Wu ET, Lu CW, Wu MH. Increased microvolt T-wave alternans in patients with repaired tetralogy of Fallot. *Int J Cardiol*. 2012;159:220–224.
2. Khairy P, Harris L, Landzberg MJ, Viswanathan S, Barlow A, Gatzoulis MA, Fernandes SM, Beauchesne L, Therrien J, Chetaille P, Gordon E, Vonder Muhll I, Cecchin F. Implantable cardioverter-defibrillators in tetralogy of Fallot. *Circulation*. 2008;117:363–370.
3. Gatzoulis MA, Balaji S, Webber SA, Siu SC, Hokanson JS, Poile C, Rosenthal M, Nakazawa M, Moller JH, Gillette PC, Webb GD, Redington AN. Risk factors for arrhythmia and sudden cardiac death late after repair of tetralogy of Fallot: a multicentre study. *Lancet*. 2000;356:975–981.
4. Gatzoulis MA, Till JA, Redington AN. Depolarization-repolarization inhomogeneity after repair of tetralogy of Fallot. The substrate for malignant ventricular tachycardia? *Circulation*. 1997;95:401–404.
5. Gatzoulis MA, Till JA, Somerville J, Redington AN. Mechanoelectrical interaction in tetralogy of Fallot. QRS prolongation relates to right ventricular size and predicts malignant ventricular arrhythmias and sudden death. *Circulation*. 1995;92:231–237.
6. Chiu SN, Wang JK, Chen HC, Lin MT, Wu ET, Chen CA, Huang SC, Chang CI, Chen YS, Chiu IS, Chen CL, Wu MH. Long-term survival and unnatural deaths of patients with repaired tetralogy of Fallot in an Asian cohort. *Circ Cardiovasc Qual Outcomes*. 2012;5:120–125.
7. Chiu SN, Wu MH, Su MJ, Wang JK, Lin MT, Chang CC, Hsu HW, Shen CT, Theriault O, Chahine M. Coexisting mutations/polymorphisms of the long QT syndrome genes in patients with repaired tetralogy of Fallot are associated with the risks of life-threatening events. *Hum Genet*. 2012;131:1295–1304.
8. Moore JP, Seki A, Shannon KM, Mandapati R, Tung R, Fishbein MC. Characterization of anatomic ventricular tachycardia isthmus pathology after surgical repair of tetralogy of Fallot. *Circ Arrhythm Electrophysiol*. 2013;6:905–911.
9. Pastore JM, Girouard SD, Laurita KR, Akar FG, Rosenbaum DS. Mechanism linking T-wave alternans to the genesis of cardiac fibrillation. *Circulation*. 1999;99:1385–1394.
10. Sato D, Shiferaw Y, Garfinkel A, Weiss JN, Qu Z, Karma A. Spatially discordant alternans in cardiac tissue: role of calcium cycling. *Circ Res*. 2006;99:520–527.
11. Wilson LD, Rosenbaum DS. Mechanisms of arrhythmogenic cardiac alternans. *Europace*. 2007;9(suppl 6):vi77–vi82.
12. Pruvot EJ, Katra RP, Rosenbaum DS, Laurita KR. Role of calcium cycling versus restitution in the mechanism of repolarization alternans. *Circ Res*. 2004;94:1083–1090.
13. Akar FG, Spragg DD, Tunin RS, Kass DA, Tomaselli GF. Mechanisms underlying conduction slowing and arrhythmogenesis in nonischemic dilated cardiomyopathy. *Circ Res*. 2004;95:717–725.
14. Chiu SN, Huang SC, Chang CW, Chen YS, Chen HC, Lin MT, Chen CA, Wang JK, Wu MH. The role of mechanical-electrical interaction in ventricular arrhythmia: evidence from a novel animal model for repaired tetralogy of Fallot. *Pediatr Res*. 2011;70:247–252.
15. Tsai CT, Chiang FT, Tseng CD, Yu CC, Wang YC, Lai LP, Hwang JJ, Lin JL. Mechanical stretch of atrial myocyte monolayer decreases sarcoplasmic reticulum calcium adenosine triphosphatase expression and increases susceptibility to repolarization alternans. *J Am Coll Cardiol*. 2011;58:2106–2115.
16. Efimov I, Salama G. The future of optical mapping is bright: RE: review on: “Optical imaging of voltage and calcium in cardiac cells and tissues” by Herron, Lee, and Jalife. *Circ Res*. 2012;110:e70–e71.
17. Herron TJ, Lee P, Jalife J. Optical imaging of voltage and calcium in cardiac cells & tissues. *Circ Res*. 2012;110:609–623.
18. Eloff BC, Lerner DL, Yamada KA, Schuessler RB, Saffitz JE, Rosenbaum DS. High resolution optical mapping reveals conduction slowing in connexin43 deficient mice. *Cardiovasc Res*. 2001;51:681–690.
19. Tsai CT, Wang DL, Chen WP, Hwang JJ, Hsieh CS, Hsu KL, Tseng CD, Lai LP, Tseng YZ, Chiang FT, Lin JL. Angiotensin II increases expression of alpha1C subunit of L-type calcium channel through a reactive oxygen species and cAMP response element-binding protein-dependent pathway in HL-1 myocytes. *Circ Res*. 2007;100:1476–1485.
20. Wilson LD, Jeyaraj D, Wan X, Hoeker GS, Said TH, Gittinger M, Laurita KR, Rosenbaum DS. Heart failure enhances susceptibility to arrhythmogenic cardiac alternans. *Heart Rhythm*. 2009;6:251–259.

21. Choi BR, Jang W, Salama G. Spatially discordant voltage alternans cause wavebreaks in ventricular fibrillation. *Heart Rhythm*. 2007;4:1057–1068.
22. Walker ML, Rosenbaum DS. Repolarization alternans: implications for the mechanism and prevention of sudden cardiac death. *Cardiovasc Res*. 2003;57:599–614.
23. Glukhov AV, Fedorov VV, Kalish PW, Ravikumar VK, Lou Q, Janks D, Schuessler RB, Moazami N, Efimov IR. Conduction remodeling in human end-stage nonischemic left ventricular cardiomyopathy. *Circulation*. 2012;125:1835–1847.
24. Watanabe M, Yokoshiki H, Mitsuyama H, Mizukami K, Ono T, Tsutsui H. Conduction and refractory disorders in the diabetic atrium. *Am J Physiol Heart Circ Physiol*. 2012;303:H86–H95.
25. Khairy P, Aboulhosn J, Gurvitz MZ, Opatowsky AR, Mongeon FP, Kay J, Valente AM, Earing MG, Lui G, Gersony DR, Cook S, Ting JG, Nickolaus MJ, Webb G, Landzberg MJ, Broberg CS; Alliance for Adult Research in Congenital C. Arrhythmia burden in adults with surgically repaired tetralogy of Fallot: a multi-institutional study. *Circulation*. 2010;122:868–875.
26. Chen CA, Tseng WY, Wang JK, Chen SY, Ni YH, Huang KC, Ho YL, Chang CI, Chiu IS, Su MY, Yu HY, Lin MT, Lu CW, Wu MH. Circulating biomarkers of collagen type I metabolism mark the right ventricular fibrosis and adverse markers of clinical outcome in adults with repaired tetralogy of Fallot. *Int J Cardiol*. 2013;167:2963–2968.
27. Moon TJ, Choueiri N, Geva T, Valente AM, Gauvreau K, Harrild DM. Relation of biventricular strain and dyssynchrony in repaired tetralogy of Fallot measured by cardiac magnetic resonance to death and sustained ventricular tachycardia. *Am J Cardiol*. 2015;115:676–680.
28. Khairy P, Landzberg MJ, Gatzoulis MA, Lucron H, Lambert J, Marcon F, Alexander ME, Walsh EP. Value of programmed ventricular stimulation after tetralogy of Fallot repair: a multicenter study. *Circulation*. 2004;109:1994–2000.
29. Pastore JM, Rosenbaum DS. Role of structural barriers in the mechanism of alternans-induced reentry. *Circ Res*. 2000;87:1157–1163.
30. Sato D, Shiferaw Y, Qu Z, Garfinkel A, Weiss JN, Karma A. Inferring the cellular origin of voltage and calcium alternans from the spatial scales of phase reversal during discordant alternans. *Biophys J*. 2007;92:L33–L35.
31. Chen PS, Ogawa M, Maruyama M, Chua SK, Chang PC, Rubart-von der Lohe M, Chen Z, Ai T, Lin SF. Imaging arrhythmogenic calcium signaling in intact hearts. *Pediatr Cardiol*. 2012;33:968–974.
32. Hayashi H, Shiferaw Y, Sato D, Nihei M, Lin SF, Chen PS, Garfinkel A, Weiss JN, Qu Z. Dynamic origin of spatially discordant alternans in cardiac tissue. *Biophys J*. 2007;92:448–460.
33. Morita H, Zipes DP, Lopshire J, Morita ST, Wu J. T wave alternans in an in vitro canine tissue model of Brugada syndrome. *Am J Physiol Heart Circ Physiol*. 2006;291:H421–H428.
34. Qu Z, Xie Y, Garfinkel A, Weiss JN. T-wave alternans and arrhythmogenesis in cardiac diseases. *Front Physiol*. 2010;1:154.
35. Luo CH, Rudy Y. A model of the ventricular cardiac action potential. Depolarization, repolarization, and their interaction. *Circ Res*. 1991;68:1501–1526.
36. Sah R, Ramirez RJ, Oudit GY, Gidrewicz D, Trivieri MG, Zobel C, Backx PH. Regulation of cardiac excitation-contraction coupling by action potential repolarization: role of the transient outward potassium current (I_{to}). *J Physiol*. 2003;546:5–18.
37. Sah R, Ramirez RJ, Backx PH. Modulation of Ca²⁺ release in cardiac myocytes by changes in repolarization rate: role of phase-1 action potential repolarization in excitation-contraction coupling. *Circ Res*. 2002;90:165–173.
38. Cordeiro JM, Calloe K, Moise NS, Kornreich B, Giannandrea D, Di Diego JM, Olesen SP, Antzelevitch C. Physiological consequences of transient outward K⁺ current activation during heart failure in the canine left ventricle. *J Mol Cell Cardiol*. 2012;52:1291–1298.
39. Dong M, Yan S, Chen Y, Niklewski PJ, Sun X, Chenault K, Wang HS. Role of the transient outward current in regulating mechanical properties of canine ventricular myocytes. *J Cardiovasc Electrophysiol*. 2010;21:697–703.
40. Kjolbye AL, Dikshteyn M, Eloff BC, Deschenes I, Rosenbaum DS. Maintenance of intercellular coupling by the antiarrhythmic peptide rotigaptide suppresses arrhythmogenic discordant alternans. *Am J Physiol Heart Circ Physiol*. 2008;294:H41–H49.
41. Aiba T, Tomaselli GF. Electrical remodeling in the failing heart. *Curr Opin Cardiol*. 2010;25:29–36.
42. Amin AS, Tan HL, Wilde AA. Cardiac ion channels in health and disease. *Heart Rhythm*. 2010;7:117–126.
43. Hui W, Slorach C, Dragulescu A, Mertens L, Bijnens B, Friedberg MK. Mechanisms of right ventricular electromechanical dyssynchrony and mechanical inefficiency in children after repair of tetralogy of Fallot. *Circ Cardiovasc Imaging*. 2014;7:610–618.
44. Benoist D, Stones R, Drinkhill MJ, Benson AP, Yang Z, Cassan C, Gilbert SH, Saint DA, Cazorla O, Steele DS, Bernus O, White E. Cardiac arrhythmia mechanisms in rats with heart failure induced by pulmonary hypertension. *Am J Physiol Heart Circ Physiol*. 2012;302:H2381–H2395.
45. Li GR, Lau CP, Ducharme A, Tardif JC, Nattel S. Transmural action potential and ionic current remodeling in ventricles of failing canine hearts. *Am J Physiol Heart Circ Physiol*. 2002;283:H1031–H1041.